Journal of Hazardous Materials 172 (2009) 289–297

Contents lists available at ScienceDirect

Journal of Hazardous Materials

journal homepage: www.elsevier.com/locate/jhazmat

Sorption of SPADNS azo dye on polystyrene anion exchangers: Equilibrium and kinetic studies

Magdalena Greluk*, Zbigniew Hubicki

Department of Inorganic Chemistry, Faculty of Chemistry, Marie Curie-Sklodowska University, 20-031 Lublin, Poland

ARTICLE INFO

Article history:
Received 23 January 2009
Received in revised form 2 July 2009
Accepted 2 July 2009
Available online 8 July 2009

Keywords:
Dye
Sorption
Kinetics
Isotherms
Anion exchanger

ABSTRACT

The sorption of SPANDS from aqueous solution onto the macroporous polystyrene anion exchangers of weakly basic Amberlyst A-21 and strongly basic Amberlyst A-29 in a batch method was studied. The effect of initial dye concentration and phase contact time was considered to evaluate the sorption capacity of anion exchangers. Equilibrium data were attempted by various adsorption isotherms including the Langmuir, Freundlich and Dubinin–Radushkevich (D–R) models. A comparison of kinetic models applied to the adsorption rate constants and equilibrium sorption capacities was made for the Lagergren first-order, pseudo second-order and Morris–Weber intraparticle diffusion kinetic models. The results showed that the adsorption isotherm is in the good agreement with the Langmuir equation and that the adsorption kinetics of SPADNS on both anion exchangers can be best described by the pseudo second-order model.

1. Introduction

Waste treatment is one of major problems facing the chemical, petrochemical, pharmaceutical and textile industries. These industries generate large quantities of organic pollutants that cause environmental and health problems [1]. Dyes are common water pollutants and they may be frequently found in trace quantities in industrial wastewater. Their presence in water, even at very low concentrations is highly visible and undesirable [2]. Over 100,000 commercially available dyes exist and more than 7×10^5 tones are produced annually. An indication of the scale of the problem is the fact that two per cent of dyes produced are discharged directly in aqueous effluents [3]. The overwhelming majority of synthetic dyes currently used are the highly water soluble azo dyes characterized by the existence of nitrogen–nitrogen double bonds and the presence of bright color is due to these azo bonds and associated chromospheres [4]. The azo dyes also contain auxochromes such as $-NH_2$, $-OH$, $-COOH$, $-SO_3H$ which are responsible for the increase of color intensity [5]. Color in the effluent is one of the most obvious indicators of water pollution and the discharge of highly colored synthetic dye effluents is aesthetically displeasing and can damage the receiving water body by impending penetration of light. Moreover, the azo dyes which are composed of ionosable groups such as sulphonates ($-SO_3^-$), carboxylates ($-CO_2^-$) are most problematic with their high molecular weight, as they tend to pass through the conventional treatment system unaffected [6,7]. The release of colored dyes into the ecosystem is a dramatic source of eutrophication, and perturbations in aquatic lives. Some azo dyes and their degradation products such as aromatic amines are highly carcinogenic [8]. The acute toxicity of azo dyes is low and may cause skin and eye irritation, weakness and dizziness. Only a few dyes showed LD_{50} values below 250 mg/kg body weight, where as the majority showed LD_{50} values between 250 and 14,000 mg/kg body weight. It is necessary to treat the industrial effluent to remove the dyes from the effluents before discharging it into hydrosphere [9].

Many different treatment techniques have been used in the removal of colored dyes from wastewater. These methods are coagulation/flocculation [4,10,11], chemical oxidation and photocatalytic processes [5,12,13], ozone treatment [14], membrane technology [15,16] and biological treatments [7,17,18]. But these processes have disadvantages and limitations, such as high cost, generation of secondary pollutants, and poor removal efficiency. Thus adsorption has been found to be the most effective economical alternative with high potential for the removal and recovery of dyes from wastewater [19]. Activated carbons used in granular, powder or fiber forms are the most common adsorbents in the liquid-phase dye adsorption process [20–23]. However, although it has a great adsorption capacity due to its highly porous structure, extremely large surface area to volume ratio and high degree of surface reactivity, it suffers from a number of disadvantages. Activated carbon is quite expensive and the higher the quality, the greater is the cost. Both chemical and thermal regeneration of spent carbon is expensive, impractical on a large scale producing additional effluent and resulting a considerable loss of adsorbent [18].

* Corresponding author. Tel.: +48 81 537 57 38; fax: +48 81 533 33 48.
E-mail address: magdalena.greluk@gmail.com (M. Greluk).

0304-3894/$ – see front matter © 2009 Elsevier B.V. All rights reserved.
doi:10.1016/j.jhazmat.2009.07.007

In recent years, many low-cost and easily obtainable natural materials such as zeolite [24–26], sepiolite [27,28], dolomite [29], alunite [30], chitin [31], oxihumolite [32] and industrial solid wastes such as fly ash [33], hydroxide sludge [34], mud [33,35], basic oxygen furnace slag [36], sawdust [37,38] as adsorbents have been tested for pollutant removal. Numerous studies have been focused on utilization of wastes from agriculture as sorbents and their application in dyes removal. Of many examples reported in literature, the following may be mentioned: soy meal hull [39], peanut hull [40], rice husk [41], coconut husk [42], kudzu [43], banana pith [44], orange peel [45,46], kohlrabi peel [47], sunflower seed shells [48]. The comparison of adsorption performance of these low-cost adsorbents is very difficult due to the lack of consistency in the literature data. Adsorption capacities were evaluated at different pH (and not necessarily at the optimum pH), temperatures and the dyes concentration ranges which makes comparison very complicated. Another very important and helpful factor in comparing these materials, namely the adsorbent cost, is seldom reported in the research papers. According to the available literature data bagasse, flyash, peat, sphagnum moss peat, fullers earth, BF slag, bentonite, zeolite, manganese oxide, laterite soil, carbonaceous adsorbent are the materials costing $\leq$0.1 US $ per kg making them useful materials in terms of cost as compared to commercial ACs which normally costs more than 1.5 US $ per kg. However, these estimates should be considered as indicative, as the cost may vary because it strongly depends on local availability, processing required, treatment conditions, and both recycle and lifetime issues. It varies depending on the fact when/where the adsorbents are made in/for developed, developing or undeveloped countries. The dye removal data available in literature suggest that removal of dyes is possible by low-cost adsorbents to a certain extent since some promising results are obtained in some of the studies. It is worth noting that some of the materials can be used as adsorbents with little or no pretreatment and can therefore be manufactured at low cost which is a great advantage for the less industrialized world. Thus, undoubtedly low-cost materials offer a lot of promising benefits for commercial purposes in the future but now their adsorption capacities, mechanical strength, and other properties need further improvement for wider application. The studies show that there is still a need for some technical improvements in preparing and especially utilizing adsorbents because it is indicated that the sorption capacity of low-cost materials is often effective only when large amount of loading of these materials is used for color removal, particularly in the case of high dye concentration, consequently producing large amount of sludge [35,49–53].

In the recent years, besides the low-cost materials polymeric adsorbents [54,55] have emerged as a potential alternative to activated carbons in terms of their vast surface area, perfect mechanical rigidity, adjustable surface chemistry and pore size distribution as well as and feasible regeneration under mild conditions. Another group of materials being alternative to the activated carbon are the commercial anion exchange resins. They have been shown to possess excellent adsorption capacity because of the functional groups bounded to the polymeric matrices which in comparison with the polymeric adsorbents additionally provide specific interactions with the target pollutants and effectively improve adsorption performance of a polymeric adsorbent toward highly water soluble dyes. Besides, the anion exchangers demonstrate efficient regeneration property for the removal and recovery of dyes which gives an important economic and environmental impetus. What is more, there is not much of a market for services for the resins, as there is for activated carbons, so suppliers generally compete on price and production cost efficiency. Prices for ion-exchange resins in the U.S. market have remained stable over the past three years following a dip through the 1990s, sources say. Prices now average between 0.24 US $ and 0.45 US $ per kg for cationic resins, and between 0.70 US $ and 0.93 US $ per kg for anionic resins [51,56,57]. Despite all these advantages of the anion exchangers, a very limited amount of information is available about their use as a method for dye removal. Karcher et al. [58] tested several commercial weakly and strongly basic anion exchangers for dye removal and found that they are very effective adsorbents. Their follow-up study provided useful information for the successes of packed-bed operation, including the aspect of resin regeneration [59]. Also Wawrzkiewicz and Hubicki [60] proved the potential application of strongly basic anion exchange resins for removal of the azo dye named tartrazine. Therefore, anion exchange resins should be a good choice for dye adsorption and the related performance should be intensively evaluated. Especially the macroporous anion exchangers derived from styrene–divinylobenzene copolymers seem to occupy a special place among the anion exchangers used in the field of dyes removal. The macroporous anion exchangers allow the penetration of large molecules of dyes inside their network as well as an easier elution during the regeneration process. However, copolymers of styrene and divinylobenzene as matrices for ion exchange resins have an excellent physical strength and resistance to the degradation by oxidation, hydrolysis or elevated temperatures. These advantages make the macroporous anion exchanger with the styrene–divinylobenzene matrix promising material for dyes removal. However, the investigation by Karcher et al. [58] proved that the adsorption capacity is dependent not only on the number and type of functional group or on the chemical and physical structures of macroporous matrix but also on the structure of organic compound. Because there exists a large variety of dyes and their removal is based on various factors, e.g. dye–anion exchanger interaction. More detailed work on these interactions between different dyes and anion exchange resins is needed for the studies to correlate and compare [50,61,62].

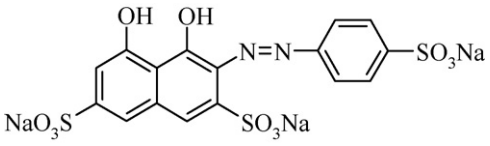

Fig. 1. Chemical structure of SPADNS.

The purpose of the present study was to screen and investigate the commercially available macroporous polystyrene anion exchange resins: Amberlyst A-21 and Amberlyst A-29 for removal of azo dye: SPADNS (2-(p-sulphophenyloazo)-1,8-dihydroxy-3,6-napthalenedisulphonic acid trisodium salt). The effects of some parameters, such as phase contact time and initial dye concentration were examined. As effective applications of sorbent require more detailed knowledge of sorption mechanism, the equilibrium isotherms and kinetic study were performed. The adsorption isotherms are described by the Freundlich, Langmuir and Dubinin–Radushkevich (D–R) isotherm models. The pseudo first-order and pseudo second-order models were tested to fit the experimental kinetic dependencies. An intraparticle diffusion model was also used to examine diffusional processes affecting the rate of dye sorption.

2. Materials and methods

2.1. Reagents

Azo dye SPADNS was purchased from POCH (Poland). The structure of dye is presented in Fig. 1. The dye was used as supplied without purification, and the fraction of inert material was not taken into account in the calculation of dye concentration.

Table 1
Physicochemical properties of the anion exchangers.

Description	Amberlyst A-21	Amberlyst A-29
Type	Weakly basic	Strongly basic
Functional groups	$-N(CH_3)_2$	$-N^+(CH_3)_2C_2H_4OH$
Matrix	Styrene divinylobenzene	
Structure	Macroporous	
Ionic form as shipped	Free base	Cl^-
Bead size [mm]	0.49–0.69	0.4–0.5
Total capacity [eq/dm^3]	≥1.25	≥0.85
Max. operating temp. [°C]	100	65
Producer	Rohm and Haas, France	Rohm and Haas, France

The macroporous resins Amberlyst A-21 and Amberlyst A-29 were used for sorption studies. The anion exchangers were supplied by Rohm and Haas (France). Important physical and chemical properties of these resins are presented in Table 1.

2.2. Apparatus

A laboratory shaker (Elphine type, Poland) was used to shake the anion exchangers and liquid phases. An UV–VIS spectrophotometer (Specord M 42, Carl Zeiss Jena, Germany) was used for absorbance measurements of the samples. The maximum wavelength (λ_{max}) used for determination of residual concentration of SPADNS in the supernatant solution using a UV–VIS spectrophotometer was 507 nm. Only the linear range of calibration curve was used in this research.

2.3. Experimental procedure

In the experiments of equilibrium adsorption isotherm, 0.2 g samples of anion exchangers were shaken mechanically in the conical flask with 20 cm^3 of SPADNS dye solution of different initial concentrations (30–12,000 mg/dm^3) for 120 min at 20 °C. In the experiments of kinetic adsorption, 0.2 g samples of anion exchangers were shaken mechanically in the conical flask with 20 cm^3 of SPADNS dye solution of different initial concentrations (57, 100, 200, 300, 500 mg/dm^3) for the period from 1 to 240 min at 20 °C.

All SPADNS solutions were filtered off to determine the content of dye in the raffinate using the spectrophotometric method. The data obtained from the adsorption tests were used to calculate the adsorption capacity, q_t (mg/dm^3) from the following Eq. (1):

$$q_e = \frac{(C_0 - C_e)}{w} \times V \quad (1)$$

where C_0 is the initial concentration of SPADNS in the aqueous phase, C_e is the concentration of SPADNS in the solutions after time t, V is the volume of the solutions (dm^3) and w is the weight of the dry anion exchanger (g).

2.4. Adsorption isotherms

Equilibrium data, commonly used as adsorption isotherms, are basic requirements for the adsorption systems under investigation. Obtaining equilibrium data for a specific sorbate/sorbent system can be performed experimentally, with a time-consuming procedure that is incompatible with the growing need for adsorption system design. They provide information on the capacity of the adsorbent or the amount of adsorbent required to adsorb a unit mass of dye under the system conditions [30,63]. Several isotherm equations are available and two of them were selected in this study. Adsorption isotherm data of SPADNS were fitted to the well-known and widely applied isotherm model of Langmuir, Freundlich and Dubinin-Radushkevich.

2.4.1. Langmuir adsorption isotherm model

The Langmuir isotherm is based on the assumption that adsorption takes place at specific homogeneous sites within the adsorbent and there is no significant interaction among the adsorbed species. It is then assumed that once a dye molecule occupies a site, no further adsorption takes place at that site. Theoretically, therefore, a saturation value is reached beyond which no further sorption takes place [30]. The linearized Langmuir isotherm equation can be written as follows:

$$\frac{C_e}{q_e} = \frac{1}{K_L} + \frac{b}{K_L} \times C_e \quad (2)$$

where q_e (mg/g) is the amount of the dye adsorbed per unit weight of the adsorbent, C_e (mg/dm^3) is the equilibrium concentration of solution, K_L (mg/g) is the monolayer adsorption capacity, b (dm^3/mg) is the Langmuir constant related with the free energy of adsorption.

When C_e/q_e is plotted against C_e and the data are regressed linearly, q_0 and b constants can be calculated from the slope and intercept.

The essential characteristic of Langmuir isotherm can be expressed by the dimensionless constant called the equilibrium parameter, R_L, defined by:

$$R_L = \frac{1}{(1 + K_L C_0)} \quad (3)$$

R_L values indicate the type of isotherm to be irreversible ($R_L = 0$), favourable ($0 < R_L < 1$), linear ($R_L = 1$) or unfavourable ($R_L > 1$) [39,63–65].

2.4.2. Freundlich adsorption isotherm model

The Freundlich isotherm model takes multilayer and heterogeneous adsorption into account. Its linearized form can be given as follows:

$$\log q_e = \log K_F + \frac{1}{n} \log C_e \quad (4)$$

where q_e and C_e have the same definitions as in the Langmuir equation above, K_F (mg/g) is the Freundlich constant related with the adsorption capacity of adsorbent and $1/n$ is another constant related with the surface heterogeneity. On this basis the latter constant sorption can be classified as irreversible ($1/n = 0$), favourable ($0 < 1/n < 1$) and unfavourable ($1/n > 1$).

When $\log q_e$ is plotted against $\log C_e$ and the data are treated by linear regression analysis, the constant K_F and the exponent n can be determined [30,39,64].

2.4.3. Dubinin–Radushkevich (D–R) adsorption isotherm model

Raduskevich and Dubnin have reported that the characteristic sorption curve is related to the porous structure of sorbent. The Dubnin-Radushkevich isotherm model, which based on the Polanyi theory, was applied to distinguish between physical and chemical adsorption. The D–R equation was given by:

$$\ln q_e = \ln X_m - \beta\varepsilon^2 \quad (5)$$

where q_e has the same definitions as in the Langmuir equation above, X_m (mg/g) is the D–R adsorption capacity, β (mol^2/kJ^2) is the activity coefficient related to the mean sorption energy and ε the Polanyi potential given by [66,67]:

$$\varepsilon = RT \ln\left(1 + \frac{1}{C_e}\right) \quad (6)$$

where R is the gas constant (kJ/mol K), C_e has the same definitions as in the above Langmuir and Freundlich equations and T is the temperature (K), when $\ln q_e$ is plotted against ε^2 and the data are treated by linear regression analysis, the constants β and q_0 can be obtained from the negative slope and the intercept, respectively.

2.5. Kinetic models of sorption

In recent years, adsorption mechanism involving kinetic models has often been reported. Numerous kinetic models have described the reaction order of adsorption system based on solution concentration.

In order to examine the controlling mechanism of sorption process such as chemical reaction, diffusion control and mass transfer, several kinetic models were used to test the experimental data [38,68].

2.5.1. Pseudo first-order equation

The pseudo first-order rate equation is generally expressed as follows:

$$\frac{dq_e}{dt} = k_1(q_1 - q_e) \tag{7}$$

where $q_1$and q_e are the amounts of dye adsorbed at equilibrium (mg/g) and at time t, respectively, and k_1 is the rate constant of pseudo first-order sorption (1/min).

After integration for the boundary conditions: $q_e = 0$ at $t = 0$ and $q_e = q_e$ at $t = t$, Eq. (7) can be rearranged to obtain a linear form:

$$\log(q_1 - q_e) = \log q_1 - \frac{k_1 t}{2.303} \tag{8}$$

A straight line of $\log(q_e - q_t)$ versus t suggests applicability of the kinetic models to fit the experimental data [30,38,69].

2.5.2. Pseudo second-order equation

The pseudo second-order chemisorption kinetic rate equation is expressed as:

$$\frac{dq_t}{dt} = k_2(q_2 - q_t)^2 \tag{9}$$

where q_2 is the amount of dye adsorbed at equilibrium (mg/g), k_2 is the equilibrium rate constant of pseudo second-order sorption (g/mg min).

Integrating Eq. (9) for the boundary conditions $q_e = 0$ at $t = 0$ and $q_e = q_e$ at $t = t$ gives:

$$\frac{t}{q_2} = \frac{1}{k_2 q_e^2} + \frac{1}{q_e} t \tag{10}$$

The initial sorption rate is:

$$h = k_2 q_e^2 \tag{11}$$

The pseudo second-order kinetic constant and the theoretical q_e are obtained from the plot of t/q_e versus t [38,60,68].

2.5.3. Weber and Morris intraparticle diffusion equation

Sorption is a multilayer process involving transport of the sorbate (dye) molecules from the aqueous phase to the surface of the solid particles, then followed by the diffusion of the solute molecules into the pore interiors. The overall adsorption process may be controlled by one or more steps, such as film or external diffusion, pore diffusion, surface diffusion and adsorption on the pore surface, or the combination of more than one step. Understanding of significance of diffusion mechanism and accurate estimates of the diffusivities of the sorbent particles are determined from the diffusion controlled kinetic models based on interpretation of the experimental data [69–71]. Due to porosity of the anion exchangers, the intraparticle diffusion was expected in the adsorption process and this was explored by using the Weber and Morris model. According to the model proposed by them, the intraparticle diffusion is commonly expressed by the following equation:

$$q_e = k_i t^{0.5} + C \tag{12}$$

Table 2
Parameters of Langmuir, Freundlich, Dubinin–Radushkevich isotherms for sorption of SPADNS on Amberlyst A-21 and Amberlyst A-29 at 20 °C.

Isotherm	Parameters	Anion exchangers	
		Amberlyst A-21	Amberlyst A-29
Langmuir	K_L (mg/g)	187.60	381.71
	b (dm^3/mg)	0.0148	0.0044
	R^2	0.999	0.970
Freundlich	K_F (mg/g)	41.99	59.40
	n	5.76	4.87
	R^2	0.969	0.953
Dubinin–Radushkevich (D–R)	X_m [mg/g]	253.26	430.82
	β [mol^2/kJ^2]	1.97×10^{-3}	2.12×10^{-3}
	E	15.92	15.34
	R^2	0.914	0.811

where k_{int} is the intraparticle diffusion rate constant (mg/g min$^{1/2}$) and C is a constant that gives information about thickness of the boundary layer [mg/g]. The k_i values are found from the slopes of q_e versus $t^{0.5}$ plots [71,72].

If the intraparticle diffusion is involved in the adsorption process, then the plot of the square root of time versus the uptake, q_e, would result in a linear relationship, and the intraparticle diffusion would be the controlling step if this line passed through the origin. When the data exhibit multi-linear plots which do not pass through the origin, this is indicative of some degree of boundary layer control and this further shows that the intraparticle diffusion is not only rate-controlling, but also other processes may control the rate of sorption [71,72].

3. Results and discussion

3.1. Adsorption isotherms

The values of the Langmuir parameters (K_L and b), Freundlich parameters (K_F, n) and Dubinin–Radushkevich parameters (X_m, β and ε) obtained from the linearized plots of the equations and the values of correlation coefficients for the SPANDS sorbed on Amberlyst A-21 and Amberlyst A-29 are listed in Table 2.

3.1.1. Langmuir adsorption isotherm

A linearized Langmuir isotherm for sorption of SPADNS on the anion exchangers: Amberlyst A-21 and Amberlyst A-29 are presented in Fig. 2. The isotherm was found to be linear over the entire concentration range studied with a good linear correlation coefficient ($R^2 = 0.998$). In both cases, the Langmuir equation represents better fit of experimental data than the other two isotherm equations.

The fact that the Langmuir isotherm fits the experimental data very well confirms the monolayer coverage of dye onto the anion exchangers and also the homogeneous distribution of active sites on them.

The Langmuir model parameters were largely dependent on the type of the investigated anion exchangers. According to this model, the monolayer saturation capacity of Amberlyst A-29 for SPADNS ($K_L = 381.71$ mg/g) was higher than those of Amberlyst A-21 for this dye ($K_L = 187.60$ mg/g). The values of sorption capacity (q_e) of Amberlyst A-21 and Amberlyst A-29 calculated using relation (1) were equal to 193.28 and 417.16 mg/dm^3, respectively and are only insignificantly different from those obtained from the Langmuir isotherm. The other Langmuir constant (b) which is related to the free energy of adsorption indicates the affinity of sorbent for binding of dye. Its value is the reciprocal of the dye concentration at which half of the saturation of the adsorbent is attained so a high value of b indicates steep desirable beginning of the isotherm

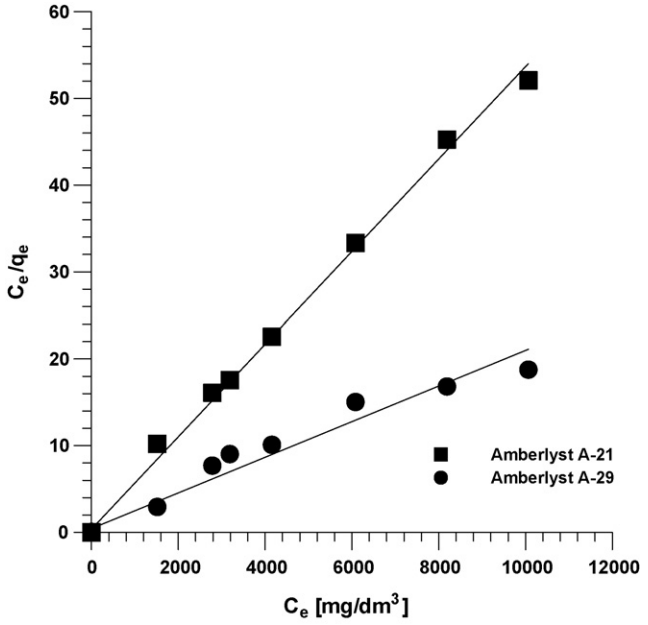

Fig. 2. Linearized forms of Langmuir isotherms for SPADNS on Amberlyst A-21 and Amberlyst A-29.

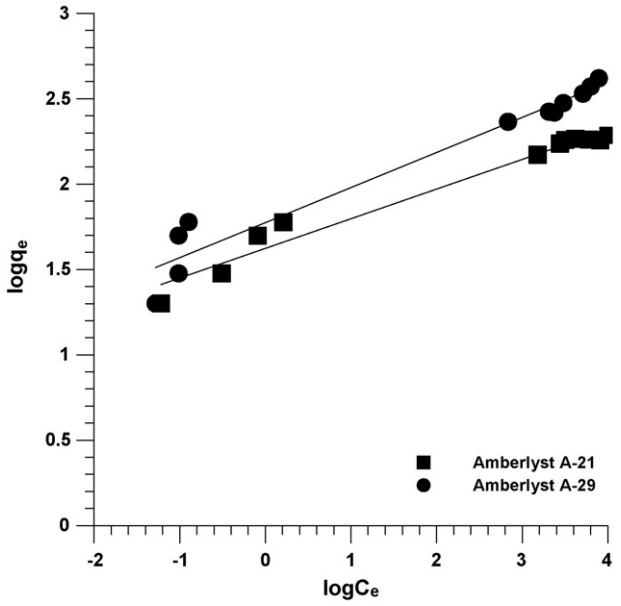

Fig. 3. Linearized forms of Freundlich isotherms for SPADNS on Amberlyst A-21 and Amberlyst A-29.

which reflects the high affinity of the anion exchangers for the sorbate resulting in a stable adsorption product [18]. The higher values of b obtained for sorption of SPANDS on Amberlyst A-21 ($b = 0.0148$) implied stronger bonding of the dye to this anion exchanger than to Amberlyst A-29 ($b = 0.0044$).

The R_L values were found to be between 4×10^{-7} and 0.13 and between 2×10^{-7} and 0.16 for different initial concentrations for the sorption of SPANDS on Amberlyst A-21 and Amberlyst A-29, respectively. The lower R_L values at higher initial SPADNS concentration showed that adsorption was more favourable at higher concentration because the degree of favourability tended toward zero rather than unity [73].

3.1.2. Freundlich adsorption isotherm

Fig. 3 shows the plot of $\log q_e$ versus $\log C_e$, the linear form of the plot indicating the fitting of experimental data to the Freundlich adsorption isotherm. The values of Freundlich correlation are lower than those of Langmuir isotherm. The Freundlich isotherm represents the poorer fit of experimental data than the Langmuir equations (Table 2).

Although the Langmuir and Freundlich constants K_L and K_F have different meanings, they lead to the same conclusion about the correlation of the experimental data of the sorption model. The basic difference between K_L and K_F is that the Langmuir isotherm assumes sorption-free energy independent of both surface coverage and formation of monolayer whereas the solid surface reaches saturation. However, the Freundlich isotherm does not predict saturation of the solid surface by adsorbate. In conclusion, K_L is the monolayer sorption capacity, while K_F is the relative sorption capacity (K_F reaches the value of q_e when the equilibrium concentration C_e approaches unity, thus being considered as an indicative parameter of the adsorption strength). A greater value of K_F indicates a higher capacity for adsorption [18,39]. As follows from Table 2, all measured values of K_F showed easy uptake of the acid dye with high adsorptive capacity of each anion exchanger. The $1/n$ values for all sorption systems studied were less than unity which reflects the favourable adsorption of SPANDS over the entire concentration range used in this study indicating a strong bond between the ion sorbed and the sorbent.

3.1.3. Dubinin–Radushkevich (D–R) adsorption isotherm

Langmuir and Freundlich isotherms are insufficient to explain the physical and chemical characteristics of adsorption. Another equation used to determine a possible adsorption mechanism is the Dubinin–Radushkevich equation, which assumes a constant sorption potential [67,74].

The D–R constants are calculated and given in Table 2. Fig. 4 shows the plot of $\ln q_e$ versus ε^2 from Eq. (5) for the uptake of SPADNS by the investigated anion exchangers. The values of coefficient of determination ($r^2 = 0.914$ for Amberlyst A-21 and $r^2 = 0.811$ Amberlyst A-29) indicate that the Dubinin–Radushkevich isotherm model does not fit well with the equilibrium data as compared with the other models considered. There were obtained linear curves were obtained whose negative slopes (β) and intercepts

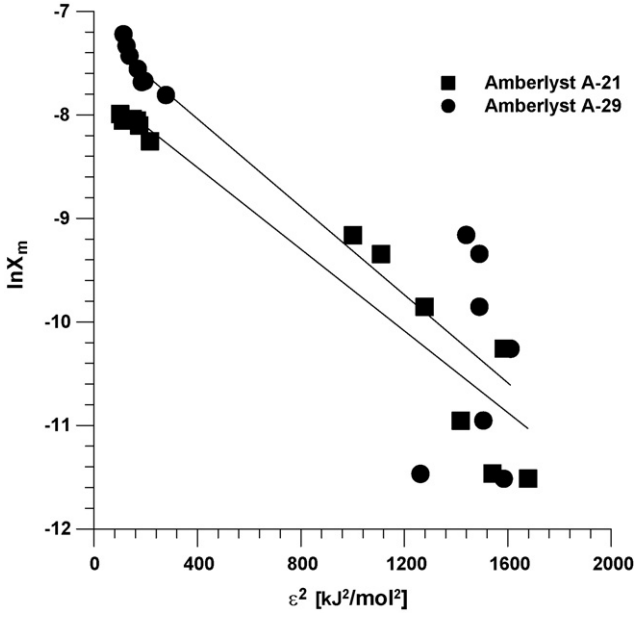

Fig. 4. Linearized forms of Dubinin–Radushkevich isotherms for SPADNS on Amberlyst A-21 and Amberlyst A-29.

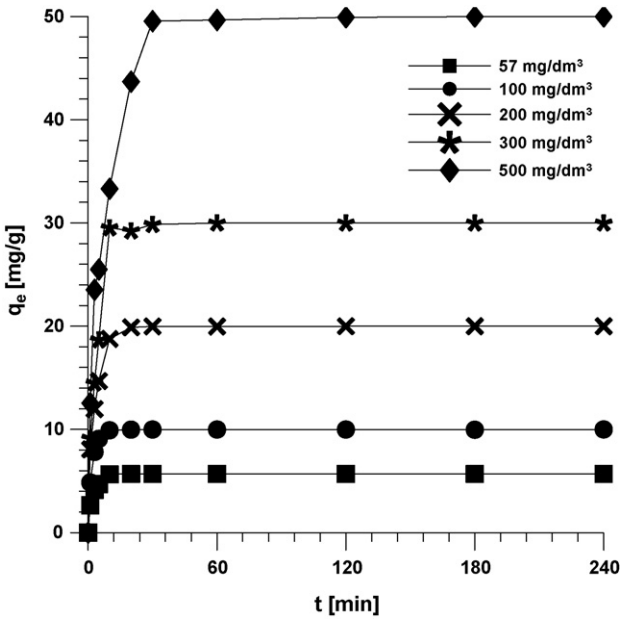

Fig. 5. Effect of the phase contact time and the initial SPADNS concentration on the sorption of dye on the weakly basic Amberlyst A-21 at 20 °C.

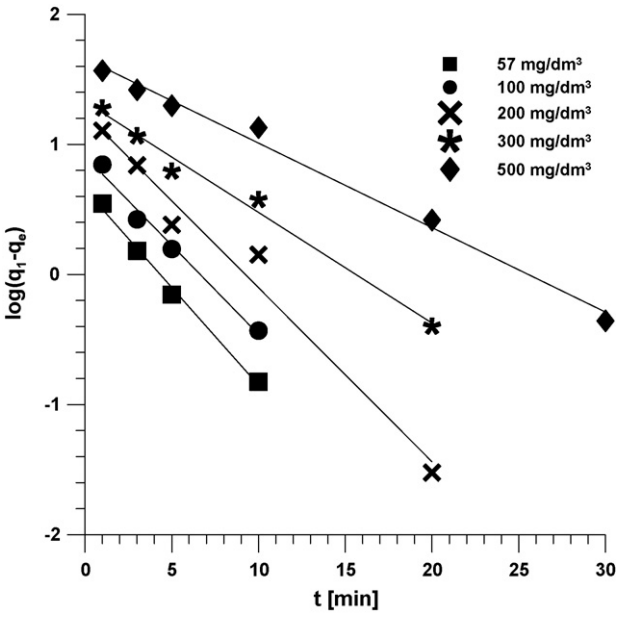

Fig. 7. Fitting of sorption kinetics of SPADNS at different initial dye concentrations on Amberlyst A-29 by means of the Lagergren model at 20 °C.

($\ln X_m$) are 1.97×10^{-3} mol^2/kJ^2 and 7.72 for Amberlyst A-21 and 2.12×10^{-3} mol^2/kJ^2 and 7.19 for Amberlyst A-29, respectively. From the preceding values, the maximum dye sorption capacities, X_m, for Amberlyst A-21 and Amberlyst A-29 were 253.26 and 430.82 mg/g respectively.

3.2. Adsorption kinetics

The values of sorption capacities (q_e) of SPADNS dye determined for the anion exchangers in question are presented in Figs. 5 and 6.

As follows from the comparison of the obtained results, the sorption capacity of dye at equilibrium on both examined anion exchangers increases from 5.69 to 49.99 mg/g with an increase in the initial dye concentration from 57 to 500 mg/dm^3.

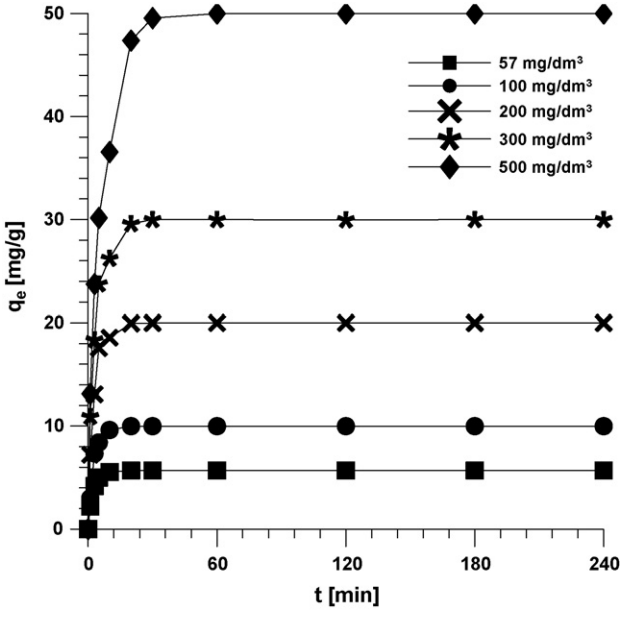

Fig. 6. Effect of the phase contact time and the initial SPADNS concentration on the sorption of dye on the weakly basic Amberlyst A-29 at 20 °C.

The equilibrium state of sorption for SPADNS occurs with the anion exchanger solution phase contact time about 10 min for the dye solutions of the initial concentration from 57 to 100 mg/dm^3. The time of contact phase necessary to reach equilibrium in the case of higher concentrations of SPADNS is longer and equals 30 min for the initial dye concentrations of 500 mg/dm^3.

3.3. Kinetic parameters

3.3.1. Pseudo first-order kinetics

Fig. 7 shows the plot $\log(q_1 - q_e)$ versus t for sorption of SPADNS for the pseudo first-order model on Amberlyst A-29. However, although the correlation coefficients, r_1^2, for the sorption of SPADNS on Amberlite A-29 were found to be higher than 0.975, the calculated equilibrium adsorption capacities $q_{e,cal}$ do not agree with the experimental values $q_{e,exp}$ (Table 3). The correlation coefficients, r_1^2, for SPADNS using Amberlyst A-21 in sorption experiments are lower and range from 0.809 to 0.999 (Table 3). Also in this case the calculated equilibrium capacities according to the pseudo first-order rate expression were not in good agreement.

As follows from Fig. 7 at all initial dye concentrations the sorption data were well represented by the first pseudo-order model only for the first 10 min when rapid sorption took place. This confirms that it is not appropriate to use the pseudo first-order model

Table 3
Pseudo first-order kinetic parameters for the effect of the initial dye concentration on the sorption of dye on Amberlyst A-21 and Amberlyst A-29 at 20 °C.

Parameters	Initial concentration				
	57 mg/dm^3	100 mg/dm^3	200 mg/dm^3	300 mg/dm^3	500 mg/dm^3
Amberlyst A-21					
$q_{e,exp}$ (mg/g)	5.69	10.00	19.99	29.99	49.99
$q_{e,cal}$ (mg/g)	6.62	2.77	16.20	16.61	51.59
k_1 (1/min)	0.487	0.214	0.248	0.169	0.141
r^2	0.961	0.884	0.999	0.809	0.929
Amberlyst A-29					
$q_{e,exp}$ (mg/g)	5.69	9.99	19.99	29.99	49.99
$q_{e,cal}$ (mg/g)	4.48	8.10	17.16	21.26	45.64
k_1 (1/min)	0.346	0.315	0.308	0.196	0.150
r^2	0.994	0.985	0.975	0.986	0.990

Table 4
Pseudo second-order kinetic parameters for the effect of the initial dye concentration on the sorption of dye on Amberlyst A-21 and Amberlyst A-29 at 20 °C.

Parameters	Initial concentration				
	57 mg/dm³	100 mg/dm³	200 mg/dm³	300 mg/dm³	500 mg/dm³
Amberlyst A-21					
$q_{e,exp}$ (mg/g)	5.69	10.00	19.99	29.99	49.99
$q_{e,cal}$ (mg/g)	5.71	10.01	20.11	30.26	50.88
k_2 (g/mg min)	0.312	0.235	0.049	0.021	0.006
h (mg/g min)	10.182	23.561	19.821	19.525	15.808
r^2	0.999	0.999	0.999	0.999	0.999
Amberlyst A-29					
$q_{e,exp}$ (mg/g)	5.69	10.00	19.99	29.99	49.99
$q_{e,cal}$ (mg/g)	5.71	10.04	20.08	30.18	50.67
k_2 (g/mg min)	0.286	0.126	0.062	0.030	0.008
h (mg/g min)	9.321	12.684	25.018	27.329	21.291
r^2	0.999	0.999	0.999	0.999	0.999

to predict the sorption kinetics of SPADNS dye on the examined anion exchangers for the entire sorption period [27].

3.3.2. Pseudo second-order kinetics

Kinetic data were further treated with the pseudo second-order kinetic model. The values of rate constant, k_2, initial sorption rate, h, equilibrium adsorption capacity, q_e, and correlation coefficient, r_2^2, were calculated and listed in Table 4. Also Fig. 8 gives the results of the linearized form of the pseudo second-order kinetic model for the sorption of SPADNS from the solution of different initial concentrations on Amberlyst A-29.

The data for Amberlyst A-21 and Amberlyst A-29 show a good compliance with the pseudo second-order equation at all initial dye concentrations studied and the correlation coefficients for the linear plots were all extremely high (>0.999). In addition, the pseudo second-order expression predicts reasonably the equilibrium sorption capacity, $q_{e,cal}$ when comparing these results with the experimental data $q_{e,exp}$. An increase in the initial dye concentration results in a significant increase of the equilibrium sorption capacity. These results suggest that the pseudo second-order sorption mechanism was predominant and the rate of each ion was controlled by chemisorption [61]. For the pseudo second-order model, the rate constant, k_2, decreases with an initial dye concentration, while the initial sorption rate, h, increases with the increasing of the initial dye concentration which can be attributed to the increase in the driving force for mass transfer, allowing more dye molecules to reach the surface of the sorbents in a shorter period of time [75].

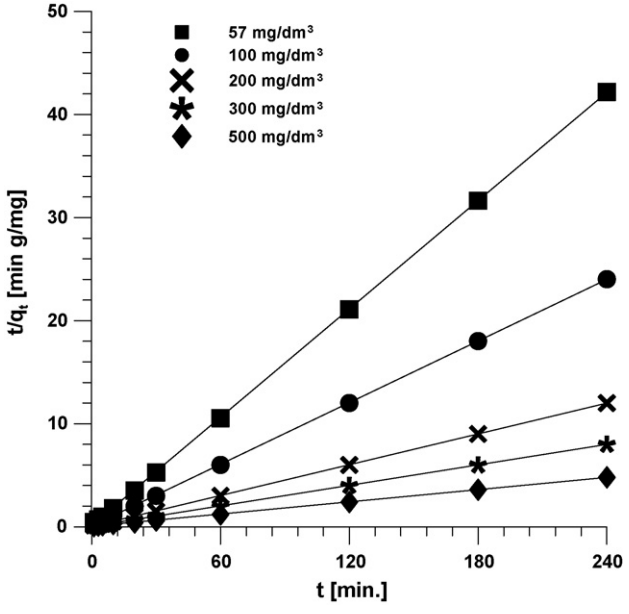

Fig. 8. Fitting of sorption kinetics of SPADNS at different initial dye concentrations on Amberlyst A-29 by means of the pseudo second-order model at 20 °C.

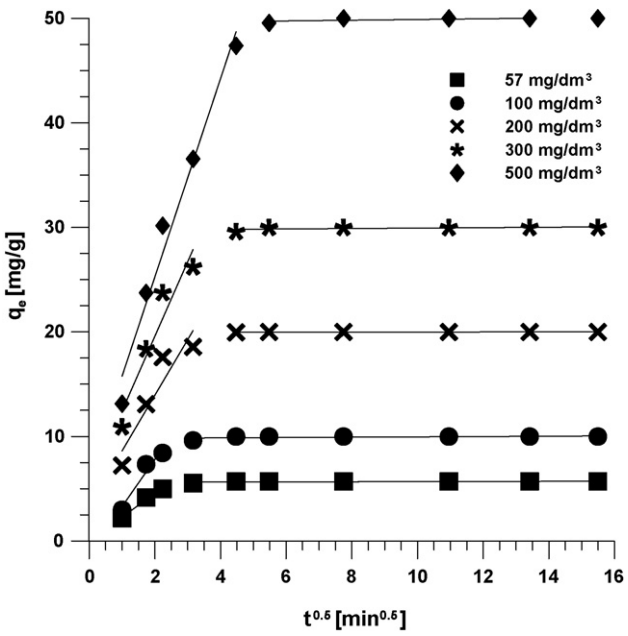

Fig. 9. Intraparticle diffusion kinetics of SPADNS at different initial dye concentrations on Amberlyst A-29 at 20 °C.

3.3.3. Weber and Morris intraparticle diffusion

Fig. 9 illustrates the intraparticle diffusion kinetics of SPADNS at various initial concentrations Amberlyst A-29. Kinetic parameters from the linear plots of this model are given in Table 5. As can be observed, the plots shown in Fig. 9 represent multi-linearity and the adsorption data could be fitted by two straight lines. The initial curved portion of the plot may be attributed to the boundary layer diffusion effect while the second linear portion is related to the intraparticle diffusion (diffusion into the polymer network) [72].

The slope of the second linear portion characterizes the rate parameter corresponding to the intraparticle diffusion, whereas the intercept of this portion is proportional to the boundary layer thickness [72].

The values of intraparticle diffusion rate constant, k_i, were found to increase from 0.002 to 0.048 mg/g min$^{1/2}$ and from 0.006 to 0.034 mg/g min$^{1/2}$ with an increase of the initial concentration of SPADNS from 57 to 500 mg/dm^3 for Amberlyst A-21 and Amberlyst A-29, respectively. This could be attributed to the driving force of diffusion. The driving force changes with the dye concentration in the bulk solution. Thus, the increase of SPADNS concentration results in an increase in the driving force, which will increase the diffusion rate of molecular dye in pores. The intraparticle coefficients, r_i^2 given in Table 5 are significantly low. Therefore, it can be suggested that SPADNS sorption on the anion exchangers Amberlyst A-21 and Amberlyst A-29 is not intraparticular diffusion control but also another mechanism is involved. Besides, the q_e versus $t^{0.5}$ plots do not pass through the origin and the values of intercepts (C in Table 5) are in the range from 5.67 to 49.31 mg/g for Amberlyst A-21 and from 5.61 to 49.54 for Amberlyst A-29. This confirms that sorption mechanism is a multi-step process which can involve adsorption on the external surface diffusion into the interior (polymer network), ion exchange and inclusion complex formation [72].

Table 5
Intraparticle diffusion parameters for the effect of the initial dye concentration on the sorption of dye on Amberlyst A-21 and Amberlyst A-29 at 20 °C.

Parameters	Initial concentration				
	57 mg/dm^3	100 mg/dm^3	200 mg/dm^3	300 mg/dm^3	500 mg/dm^3
Amberlyst A-21					
k_{int} (mg/g min$^{1/2}$)	0.002	0.003	0.007	0.046	0.048
C (mg/g)	5.67	9.95	19.90	29.39	49.31
r^2	0.266	0.278	0.450	0.526	0.921
Amberlyst A-29					
k_{int} (mg/g min$^{1/2}$)	0.006	0.015	0.002	0.021	0.034
C (mg/g)	5.61	9.80	19.97	29.72	49.54
r^2	0.334	0.334	0.371	0.453	0.567

Moreover, the values of intercept give an idea about the boundary layer effect. Namely, any increase in the value of constant C indicates the abundance of solute adsorbed on the boundary effect. The constant C is found to increase with the increasing of thickness of the boundary layer which indicates smaller probability of internal mass transfer [69].

4. Conclusion

- The investigations show that the macroporous anion exchangers with the polystyrene skeleton: Amberlyst A-21 (weakly basic) and Amberlyst A-29 (strongly basic) adsorb SPADNS azo dye with high affinity and capacity and can be used as the adsorbent for removal of this dye from aqueous solutions.
- The sorption performance is affected by various parameters, i.e. the phase contact time and the initial dye concentration.
- The kinetic data fit very well with the pseudo second-order kinetic model so sorption of SPADNS azo dye on the investigated anion exchangers can be described as the chemisorption involving valency forces through the sharing or exchanging of electrons between the adsorbent and the adsorbate as covalent forces and ion exchange.
- The equilibrium data fit well with the Langmuir isotherm model so the sorption of SPADNS on the anion exchangers is found as monolayer sorption of SPADNS molecules on the homogeneous surfaces of the anion exchangers.

References

[1] I.A. Salem, Activation of H_2O_2 by Amberlyst-15 resin supported with copper(II)-complexes towards oxidation of crystal violet, Chemosphere 44 (2001) 1109–1119.
[2] G. Crini, Studies on adsorption of dyes on beta-cyclodextrin polymer, Bioresour. Technol. 90 (2003) 193–198.
[3] G. Crini, Non-conventional low-cost adsorbents for dye removal: a review, Bioresour. Technol. 97 (2006) 1061–1085.
[4] J.W. Lee, S.P. Choi, R. Thiruvenkatachari, W.G. Shim, H. Moon, Evaluation of the performance of adsorption and coagulation process for the maximum removal of reactive dyes, Dyes Pigments 69 (2006) 196–203.
[5] I.H. Cho, K.D. Zoch, Photocatalytic degradation of azo dye (*Reactive Red 120*) in TiO_2/UV system: optimization and modeling using response surface methodology (RSM) based on the central composite design, Dyes Pigments 75 (2007) 533–543.
[6] M.S. Khehra, H.S. Saini, D.K. Sharma, B.S. Chadha, S.S. Chimni, Biodegradation of azo dye C. I. Acid Red 88 by an anoxic-aerobic sequential bioreactor, Dyes Pigments 70 (2006) 1–7.
[7] A. Özer, G. Akkaya, M. Turabik, The removal of Acid Red 274 from wastewater: combined biosorption and biocoagulation with *Spirogyra rhizopus*, Dyes Pigments 71 (2006) 83–89.
[8] M.M. Mohamed, Acid dye removal: comparison of surfactant-modified mesopororous FSM-16 with activated carbon derived from rice husk, J. Colloid Interface Sci. 272 (2004) 28–34.
[9] M. Saleem, T. Pirzada, R. Qadeer, Sorption of acid violet and direct red 80 dyes on cotton fiber from aqueous solutions, Colloids Surf. A 292 (2007) 246–250.
[10] T.H. Kim, C. Park, J. Yang, S. Kim, Comparison of disperse and reactive dye removals by chemical coagulation and Fenton oxidation, J. Hazard. Mater. 112 (2004) 2041–2065.
[11] V. Golob, A. Vinder, M. Simonič, Efficiency of the coagulation/flocculation method for the treatment of dyebath effluents, Dyes Pigments 67 (2005) 93–97.
[12] J. Bandara, J. Nadtochenko, J. Kiwi, C. Pulgarin, Dynamics of oxidant addition as a parameter in the modelling of dye mineralization (Orange II) via advanced oxidant technologies, Water Sci. Technol. 35 (1997) 87–93.
[13] S.M. Tsui, W. Chu, Photocatalytic degradation of dye pollutants in the presence of acetone, Water Sci. Technol. 44 (2001) 173–180.
[14] J.N. Wu, T.W. Wang, effects of some water-quality and operating parameters on the decolarization of reactive dye solutions by ozone, J. Environ. Sci. Health, Part A 36 (2001) 1335–1347.
[15] T.H. Kim, C. Park, S. Kim, Water recycling from desalination and purification process of reactive dye manufacturing industry by combined membrane filtration, J. Cleaner Prod. 13 (2005) 779–786.
[16] I. Koyuncu, Reactive dye removal in dye/salt mixtures by nanofiltration membranes containing vinylosulphone dyes: effects of feed concentration and cross flow velocity, Desalination 143 (2002) 243–253.
[17] M.Y. Arica, G. Bayramoğlu, Biosorption of Reactive Red-120 dye from aqueous solution by native and modified fungus biomass preparations of *Lentinus sajor-caju*, J. Hazard. Mater. 149 (2007) 499–507.
[18] Z. Aksu, A.İ. That, Ö. Tunç, A comperative adsorption/biosorption study of Acid Blue 161: effect of temperature on equilibrium and kinetic parameters, Chem. Eng. J. 142 (2008) 23–39.
[19] X. Jin, M. Jiang, X. Shan, Z. Pei, Z. Chen, Adsorption of methylene blue and orange II onto unmodified and surfactant-modified zeolite, J. Colloid Interface Sci. 328 (2008) 243–247.
[20] Y. Al-Degs, M. Khraisheh, S. Allen, M. Ahmad, Effect of carbon surface chemistry on the removal of reactive dyes from textile effluents, Water Res. 34 (2000) 927–935.
[21] V. Meshko, L. Markovska, M. Mincheva, A.E. Rodrigues, Adsorption of basic dyes on granular activated carbon and natural zeolite, Water Res. 35 (2001) 3357–3366.
[22] X. Yang, B. Al-Duri, Kinetic modeling of liquid-phase adsorption of reactive dyes on activated carbon, J. Colloid Interface Sci. 287 (2005) 25–34.
[23] Y.S. Al-Degs, M.I. El-Barghouthi, A.H. El-Sheikh, G.M. Walker, Effect of solution pH, ionic strength, and temperature on adsorption behavior of reactive dyes on activated carbon, Dyes Pigments 77 (2008) 16–23.
[24] Y.E. Benkli, M.F. Can, M. Turan, M.S. Çelik, Modificatiom of organo-zeolite surface for the removal of reactive azo dyes in fixed-bed reactors, Water Res. 39 (2005) 487–493.
[25] D. Karadag, M. Turan, E. Akgul, S. Tok, A. Faki, Adsorption equillibrium and kinetics of Reactive Black 5 and Reactive Red 239 in aqueous solution onto surfactant-modified zeolite, J. Chem. Eng. Data 52 (2007) 1615–1620.
[26] A.B. Engin, Ö. Özdemir, M. Turan, A.Z. Turan, Color removal from textile dyebath effluents in a zeolite fixed bed reactor: determination of optimum process conditions using Taguchi method, J. Hazard. Mater. 159 (2008) 348–353.
[27] M. Alkan, Ö. Demirbas, S. Celikçapa, M. Dogan, Sorption of acid red 57 from aqueous solutions onto sepiolite, J. Hazard. Mater. 116 (2004) 135–145.
[28] M. Alkan, S. Celikçapa, Ö. Demirbas, M. Dogan, Removal of reactive blue 221 and acid blue 62 anionic dyes from aqueous solutions by sepiolite, Dyes Pigments 65 (2005) 251–259.
[29] G.M. Walker, L. Hansen, J.A. Hanna, S.J. Allen, Kinetics of reactvive dye adsorption onto dolomitic sorbents, Water Res. 27 (2003) 2081–2089.
[30] M. Özacar, İ.A. Şengil, Adsorption of reactive dyes on calcined alunite from aqueous solutions, J. Hazard. Mater. B98 (2003) 211–224.
[31] G. Annadurai, M.R.V. Krishnan, Adsorption of acid dye from aqueous solution by chitin: equilibrium studies, Indian J. Chem. Tech. 4 (1997) 217–222.
[32] P. Janoš, P. Michálek, L. Turek, Sorption of ionic dyes onto untreated low-rank coal-oxihumolite: a kinetic study, Dyes Pigments 74 (2007) 363–370.
[33] S. Wang, Y. Boyjoo, A. Choueib, Z.H. Zhu, Removal of dyes from aqueous solution using fly ash and red mud, Water Res. 39 (2005) 129–138.
[34] S. Netpradit, P. Thiravetyan, S. Towprayoon, Adsorption of three azo reactive dyes by metal hydroxide sludge: effect of temperature, pH, and electrolytes, J. Colloid Interface Sci. 270 (2004) 255–261.
[35] M.X. Zhu, L. Lee, H.H. Wang, Z. Wang, Removal of an anionic dye by adsorption/precipitation processes using alkaline white mud, J. Hazard. Mater. 149 (2007) 735–741.
[36] Y. Xue, H. Hou, S. Zhu, Adsorption removal of reactive dyes from aqueous solution by modified basic oxygen furnace slag: isotherm and kinetic study, Chem. Eng. J. (2008), doi:10.1016/j.cej.2008.07.017.

[37] V.K. Garg, R. Gupta, A. Bala Yadav, R. Kumar, Dye removal from aqueous solution by adsorption on treated sawdust, Bioresour. Technol. 89 (2003) 121–124.
[38] M. Özacar, İ.A. Şengil, A kinetic study of metal complex dye sorption onto pine sawdust, Process Biochem. 40 (2005) 565–572.
[39] M. Arami, N.Y. Limaee, N.M. Mahmoodi, N.S. Tabrizi, Equilibrium and kinetics studies for the adsorption of direct and acid dyes from aqueous solution by soy meal hull, J. Hazard. Mater. B135 (2006) 171–179.
[40] R. Gong, M. li, C. Yang, Y. Sun, J. Chen, Removal of cationic dyes from aqueous solution by adsorption on peanut hull, J. Hazard. Mater. B121 (2005) 247–250.
[41] K.V. Kumar, S. Sivanesan, Pseudo second order kinetic models for safranin onto rice husk: comparison of linear and non-linear regression analysis, Process Biochem. 41 (2006) 1198–1202.
[42] K.S. Low, C.K. Lee, K.L. Lee, Removal of reactive dyes quaterniced coconut husk, J. Environ. Sci. Health, Part A Tox. Hazard. Subst. 33 (1998) 1479–1489.
[43] S.J. Allen, Q. Gan, R. Matthews, P.A. Johnson, Comparison of optimized models for basic dye adsorption by kudzu, Bioresour. Technol. 88 (2003) 143–152.
[44] C. Namasivayam, N. Kanchana, Waste banana pith as adsorbent for colour removal from wastewaters, Chemosphere 25 (1992) 1691–1705.
[45] C. Namasivayam, N. Muniasarny, K. Gayathri, M. Rani, K. Ranganathan, Removal of dyes from aqueous solutions by cellulosic orange peel, Bioresour. Technol. 57 (1996) 37–43.
[46] G. Annadurai, R.S. Juang, D.J. Lee, Use of cellulose-based wastes for adsorption of dyes from aqueous solutions, J. Hazard. Mater. 92 (2002) 451–455.
[47] R. Gong, X. Zhang, H. Liu, Y. Sun, B. Liu, Uptake of cationic dyes from aqueous solution by biosorption onto granular kohlrabi peel, Bioresour. Technol. 98 (2007) 1319–1323.
[48] J.F. Osma, V. Saravia, J.L. Toca-Herrera, S. Rodríguez Couto, Sunflower seed shells: a novel and effective low-cost adsorbent for the removal of diazo dye reactive Black 5 from aqueous solutions, J. Hazard. Mater. 147 (2007) 900–905.
[49] S.H. Lin, R.S. Juang, Adsorption of phenol and its derivatives from water using synthetic resins and low-cost natural adsorbents: a review, J. Environ. Manage. 90 (2009) 1336–1349.
[50] V.K. Gupta, I. Suhas, Application of low-cost adsorbents for dye removal—a review, J. Environ. Manage. (2009), doi:10.1016/j.jenvman.2008.11.017.
[51] B. Pan, B. Pan, W. Zhang, L. Lv, Q. Zhang, S. Zheng, Development of polymeric and polimer-based hybryd adsorbents for pollutants removal from wastewaters, Chem. Eng. J. (2009), doi:10.1016/j.cej.2009.02.036.
[52] A. Faki, M. Turan, O. Ozdemir, A.Z. Turan, Analysis of fixed-bed kolumn adsorption of reactive yellow 176 onto surfactant-modified zeolite, Ind. Eng. Chem. Res. 47 (2008) 6999–7004.
[53] S.K. Maji, S. Pal, T. Pal, A. Adak, Modeling and fixed bed column adsorption of As(III) on laterite soil, Sep. Purif. Technol. 56 (2007) 284–290.
[54] J. Fan, A. Li, W. Yang, L. Yang, Q. Zhang, Adsorption of water soluble dye onto styrene and acrylic ester resin, Sep. Purif. Technol. 51 (2006) 338–344.
[55] Y. Yu, Y.Y. Zhuang, Z.H. Wang, M.Q. Qiu, Adsorption of water-soluble dyes onto resin NKZ, Ind. Eng. Chem. Res. 42 (2003) 6898–6903.
[56] J.S. Wu, C.H. Liu, K.H. Chu, S.Y. Suen, Removal of cationic dye methyl violet 2B from water by cation exchange membranes, J. Membr. Sci. 309 (2008) 239–245.
[57] R. Mullin, Basic materials keep a technology edge, C&EN 80 (2002) 44–48.
[58] S. Karcher, A. Kornmüller, M. Jekel, Screening of commercial sorbents for the removal of reactive dyes, Dyes Pigments 51 (2001) 111–125.
[59] S. Karcher, A. Kornmüller, M. Jekel, Anion exchange resins for the removal of reactive dyes from textile wastewaters, Water Res. 36 (2002) 417–424.
[60] M. Wawrzkiewicz, Z. Hubicki, Removal of tartrazine from aqueous solutions by strongly basic polystyrene anion exchange resins, J. Hazard. Mater. (2008), doi:10.1016/j.jhazmat.2008.08.021.
[61] S. Dragan, M. Cristea, A. Airinei, I. Poinescu, C. Luca, Sorption of aromatic compounds on macroporous anion exchangers based on polyacryloamide: relation between structure and sorption behavior, J. Appl. Polym. Sci. 55 (1995) 421–430.
[62] Z. Hubicki, M. Leszczyńska, Studies of sorption of Pd(II) microquantities on strongly basic polyacrylate anion exchangers, Desalination 175 (2005) 289–295.
[63] K.K.H. Choy, G. McKay, J.F. Porter, Sorption of acid dyes from effluents using activated carbon, Res. Conserv. Recycl. 27 (1999) 57–71.
[64] X. Wu, D. Wu, R. Fu, Studies on the adsorption of reactive brilliant red X-3B dye on organic and carbon aerogels, J. Hazard. Mater. 147 (2007) 1028–1036.
[65] E.A. El-Sofany, Removal of lanthanum and gadolinium from nitrate medium using Aliquat-336 impregnated onto Amberlite XAD-4, J. Hazard. Mater. 153 (2008) 948–954.
[66] S. Samataya, N. Kabay, Ü. Yüksel, M. Ardam, M. Yüksel, Removal of nitrate from aqueous solution by nitrate selective ion exchange resins, React. Funct. Polym. 66 (2006) 1206–1214.
[67] S. Veli, B. Alyüz, Adsortpion of copper and zinc from aqueous solutions by using natural clay, J. Hazard. Mater. 149 (2007) 226–233.
[68] Y.S. Ho, G. McKay, Sorption of dye from aqueous solution by peat, Chem. Eng. J. 70 (1998) 115–124.
[69] A. Khaled, A. El Nemr, A. El-Sikaily, O. Abdewahab, Removal of Direct N Blue-106 from artificial textile dye effluent using activated carbon from orange peel: adsorption isotherm and kinetic studies, J. Hazard. Mater. 165 (2009) 100–110.
[70] N. Dizge, E. Demirbas, M. Kobya, Removal of thiocyanyte from aqueous solutions by ion exchange, J. Hazard. Mater. 166 (2009) 1367–1376.
[71] M.S. Biligli, Adsorption of 4-chlorophenol from aqueous solutions by xad-4 resin: isotherm, kinetic, and thermodynamic analysis, J. Hazard. Mater. B137 (2006) 157–164.
[72] G. Crini, H.N. Peindy, F. Gimbert, C. Robert, Removal of C. I. Basic green 4 (Malachite Green) from aqueous solutions by adsorption using cyclodextrin-based adsorbent: kinetic and equilibrium studies, Sep. Purif. Technol. 53 (2007) 97–110.
[73] E. Bulut, M. Özacar, İ.A. Şengil, Adsorption of malachite green onto bentonite: equilibrium and kinetic studies and process design, Microporous Mesoporous Mater. 115 (2008) 234–246.
[74] A.R. Cestari, E.F.S. Vieira, G.S. Vieira, L.E. Almeida, Aggregation and adsorption of reactive dyes in the presence of an anionic surfactant on mesoporous aminopropyl silica, J. Colloid Interface Sci. 309 (2007) 402–411.
[75] E. Demirbas, M.Z. Nas, Batch kinetic and equilibrium studies of adsorption of Reactive Blue 21 by fly ash and sepiolite, Desalination 243 (2009) 8–21.